



Published in final edited form as:

J Allergy Clin Immunol. 2018 September ; 142(3): 928–941.e8. doi:10.1016/j.jaci.2017.11.015.

Efficacy of lentivirus-mediated gene therapy in an Omenn syndrome recombination-activating gene 2 mouse model is not hindered by inflammation and immune dysregulation

Valentina Capo, PhD^a, Maria Carmina Castiello, PhD^a, Elena Fontana, PhD^{b,d}, Sara Penna, MSc^a, Marita Bosticardo, PhD^a, Elena Draghici, MSc^a, Luigi P. Poliani, MD, PhD^c, Lucia Sergi Sergi, MSc^a, Rosita Rigoni, MSc^{b,d}, Barbara Cassani, PhD^{b,d}, Monica Zanussi, BSc^e, Paola Carrera, PhD^e, Paolo Uva, PhD^f, Kerry Dobbs, MSc^g, Nicolò Sacchetti, BSc^{a,h}, Luigi D. Notarangelo, MD^g, Niek P. van Til, PhD^{i,j}, Gerard Wagemaker, PhD^{i,k,l}, and Anna Villa, MD^{a,d}

^aSan Raffaele Telethon Institute for Gene Therapy (TIGET), Division of Regenerative Medicine, Stem Cells and Gene Therapy, San Raffaele Scientific Institute, Milan;

^bHumanitas Clinical and Research Center, Rozzano, Milan;

^cInstitute of Molecular Medicine “A. Nocivelli,” University Hospital “Spedali Civili,” Brescia;

^dMilan Unit, Istituto di Ricerca Genetica e Biomedica, Consiglio Nazionale delle Ricerche, Milan;

^eGenomics for the Diagnosis of Human Pathologies, San Raffaele Scientific Institute, Milan;

^fCRS4, Science and Technology Park Polaris, Pula;

^gLaboratory of Host Defenses, National Institute of Allergy and Infectious Diseases, National Institutes of Health, Bethesda;

^hVita-Salute San Raffaele University, Milan;

ⁱDepartment of Hematology, Erasmus University Medical Center, Rotterdam;

^jLaboratory of Translational Immunology, University Medical Center Utrecht;

^kStem Cell Research and Development Center, Hacettepe University, Ankara;

^lRaisa Gorbacheva Memorial Research Institute for Pediatric Oncology and Hematology, Saint Petersburg.

Abstract

Background: Omenn syndrome (OS) is a rare severe combined immunodeficiency associated with autoimmunity and caused by defects in lymphoid-specific V(D)J recombination. Most patients carry hypomorphic mutations in recombination-activating gene (RAG) 1 or 2. Hematopoietic stem cell transplantation is the standard treatment; however, gene therapy (GT) might represent a valid alternative, especially for patients lacking a matched donor.

Objective: We sought to determine the efficacy of lentiviral vector (LV)-mediated GT in the murine model of OS (*Rag2*^{R229Q/R229Q}) in correcting immunodeficiency and autoimmunity.

Methods: Lineage-negative cells from mice with OS were transduced with an LV encoding the human *RAG2* gene and injected into irradiated recipients with OS. Control mice underwent transplantation with wild-type or OS-untransduced lineage-negative cells. Immunophenotyping, T-dependent and T-independent antigen challenge, immune spectratyping, autoantibody detection, and detailed tissue immunohistochemical analyses were performed.

Results: LV-mediated GT allowed immunologic reconstitution, although it was suboptimal compared with that seen in wild-type bone marrow (BM)2transplanted OS mice in peripheral blood and hematopoietic organs, such as the BM, thymus, and spleen. We observed *in vivo* variability in the efficacy of GT correlating with the levels of transduction achieved. Immunoglobulin levels and T-cell repertoire normalized, and gene-corrected mice responded properly to challenges *in vivo*. Autoimmune manifestations, such as skin infiltration and autoantibodies, dramatically improved in GT mice with a vector copy number/genome higher than 1 in the BM and 2 in the thymus.

Conclusions: Our data show that LV-mediated GT for patients with OS significantly ameliorates the immunodeficiency, even in an inflammatory environment.

Keywords

Gene therapy; Omenn syndrome; autoimmunity; lentiviral vector; *Rag* genes

Genetic defects in recombination-activating gene (*RAG*) 1 or 2 result in a spectrum of severe immune defects ranging from a profound block in T- and B-cell differentiation (T⁻B⁻severe combined immunodeficiency [SCID] forms) to the presence of oligoclonal lymphocytes, a condition referred to as “atypical” or leaky SCID.¹ In recent years, whole-exome sequencing has identified *RAG* mutations in late childhood or young adulthood, presenting a broad spectrum of clinical manifestations, including combined immunodeficiency associated with granulomas and/or autoimmunity or expansion of T-cell receptor (TCR) $\gamma\delta$ T cells and variable antibody deficiency.^{1–5} Hypomorphic mutations also cause a distinct clinical phenotype, Omenn syndrome (OS), in which immunodeficiency associates with the presence of eosinophilia and early-onset erythroderma caused by infiltration of oligoclonal activated T cells.^{6–8} Although circulating B cells are virtually absent, plasmablasts might be present in peripheral tissues and contribute to the pathogenesis of immune dysregulation, as revealed by the presence of autoantibodies.^{9–11} Because all these forms are fatal if untreated, hematopoietic stem cell transplantation (HSCT) is the standard of care, even in SCID diagnosed late.

The average overall survival for patients with SCID treated early in infancy is greater than 90% at 3 years after transplantation.^{12–17} Poor overall survival has been reported after haploidentical HSCT with no or limited conditioning, clearly indicating that myeloablative conditioning is required to achieve long-term T- and B-cell recovery.¹⁸

Given the encouraging results of gene therapy (GT) studies obtained in the setting of X-linked SCID^{19,20} and in adenosine deaminase deficiency,^{21,22} the GT approach represents an

attractive therapeutic option for patients with OS. Preclinical studies in the *Rag1*^{-/-} model indicated that low RAG1 expression resulted in incomplete thymic reconstitution and consequent development of OS manifestations²³ or in very low T- and B-cell counts.²⁴ The preclinical model of *Rag2*^{-/-}GT provided more encouraging data, showing amelioration of the immunodeficiency in the absence of side effects with both retroviral and lentiviral vectors (LVs).^{25,26} Significant improvement in T- and B-cell reconstitution was observed by using an LV carrying codon-optimized human *RAG2* cDNA under the control of ubiquitous chromatin opening element (UCOE) promoter (UCOE-RAG2co). Nonetheless, it remains unclear whether the same therapeutic strategy could be effective in the presence of hypomorphic *RAG2* mutations, in which gene-corrected lymphoid progenitors compete with endogenous uncorrected lymphocytes in an inflammatory and autoimmune environment.

Here we tested the UCOE-RAG2co LV in the OS preclinical model (*Rag2*^{R229Q/R229Q} mouse)²⁷ to evaluate the efficacy of a lentivirus-mediated GT approach. We demonstrated that adequate transgene expression is required to overcome T- and B-cell differentiation block and restore thymic epithelial structure. GT-treated mice showed dramatic amelioration in peripheral tissue infiltration, particularly in the skin, and antigen-specific antibody production on *in vivo* challenges. In summary, our data demonstrated the feasibility of the lentiviral GT approach, even in the context of residual RAG2 expression and, more importantly, in an inflammatory environment predisposing to autoimmunity.

METHODS

LV production

The 2.6kbUCOE-RAG2co LV, in which the human codon-optimized *RAG2* cDNA was driven by a 2.6kbUCOE, was produced as previously described.²⁶ For the 2.2kb UCOE-RAG2co LV, the 2.6kbUCOE was replaced by a shorter 2.2kbUCOE form.²⁸

Animals

Animal experimental procedures were approved by the Institutional Animal Care and Use Committee of San Raffaele Hospital and Italian Ministry of Health (Institutional Animal Care and Use Committee no. 710). C57Bl/6 wild-type (WT) mice were obtained from Charles River (Bar Harbor, Me). The knock-in C57BL/6 *Rag2*^{R229Q/R229Q} colony was maintained onsite with heterozygous breeders.²⁷

Lineage-negative transduction and transplantation

Six- to 10-week-old donor WT or *Rag2*^{R229Q/R229Q} (OS) mice were euthanized, and femurs and tibias were flushed to collect bone marrow (BM). Lineage-negative (Lin⁻) cells were enriched from total BM with the Lineage Cell Depletion Kit and autoMACS separator (Miltenyi Biotec, Bergisch Gladbach, Germany), according to the manufacturer's instructions. OS Lin⁻ cells were transduced overnight with LVs at a multiplicity of infection of 5 to 10 (vector titer, 1.3–3.8 × 10⁸ transducing units per mL) in StemSpan SFEM medium (STEMCELL Technologies, Vancouver, British Columbia, Canada) supplemented with 2% FCS (Euroclone, Milan, Italy), 1% penicillin/streptomycin, 1% glutamine (Gibco, Carlsbad, Calif), and the following cytokines (PeproTech, Rocky Hills, NJ): recombinant

murine thrombopoietin, 20 ng/mL; recombinant murine stem cell factor, 50 ng/mL; rhFLT3L, 10 ng/mL; rmIL-3, 10 ng/mL; and rhIL-6, 20 ng/mL. Untransduced Lin⁻ cells from mice with OS and WT mice were cultured in parallel in the same medium. Recipient mice were conditioned by using lethal total-body irradiation (900 rad, split dose) at least 2 hours before transplantation and were then injected in the caudal vein with 0.5×10^6 Lin⁻ cells. Donors and recipients were mismatched by sex or CD45 alleles to follow-up chimerism. Gentamicin sulfate (Italfarmaco, Milan, Italy) was administered in drinking water (8 mg/mL) for the first 2 weeks after transplantation to prevent infections.

Flow cytometric analysis

Single-cell suspensions from tissues were obtained, as previously described.²⁹ Cells were stained with the following antibodies (BD Phar-Mingen, San Jose, Calif; Miltenyi Biotec; BioLegend, San Diego, Calif; or eBioscience, San Diego, Calif): CD3, CD4, CD8, CD11b, CD19, CD21, CD23, CD24, CD25, CD43, CD44, CD45.1/2, CD62 ligand, CD69, CD117, B220, IgM, IgD, NKp46, NK1.1, Lin⁺ cocktail, and Sca1. Viability was determined by using the Live/Dead Fixable Dead Cell Stain Kit (Thermo Fisher Scientific, Waltham, Mass). Samples were acquired on a FACSCanto II (BD) and analyzed with FlowJo software (TreeStar, Ashland, Ore).

Real-time quantitative PCR

Genomic DNA was extracted with the QIAamp DNA Blood Mini Kit (Qiagen, Hilden, Germany), according to the manufacturer's instructions. Vector copy number/genome (VCN) was quantified by using quantitative real-time PCR on the Vii7 PCR System (Applied Biosystems, Foster City, Calif), as previously described.³⁰ For digital droplet PCR, 20 ng of genomic DNA was analyzed with the QX200 Droplet Digital PCR System (Bio-Rad Laboratories, Hercules, Calif), according to the manufacturer's instructions, with the same set of primers and probes used for real-time PCR and the Rpp30 gene (Bio-Rad Laboratories) as a normalizer. Chimerism in sex-mismatched transplants was evaluated by means of quantification of cells carrying the Y chromosome, as previously described.³¹

Gene expression analysis

Total RNA was obtained from spleen cells with the RNeasy Mini Kit (Qiagen) and reverse-transcribed with High-Capacity cDNA Reverse Transcription Kit (Applied Biosystems), according to the manufacturer's instructions. Vector-driven human recoded *RAG2* gene expression was analyzed with the Custom Plus TaqMan RNA assay and normalized to hypoxanthine phosphoribosyltransferase (*HPRT*) gene expression (Single Tube TaqMan Gene Expression Assay; Applied Biosystems).

Immunoglobulin and cytokine quantification

Total IgA, IgG, and IgM levels were quantified on serum samples obtained at the time of 28 weeks by using the MILLIPLEX MAP Mouse Immunoglobulin Isotyping Magnetic Bead Panel and MAGPIX System (Merck Millipore, Burlington, Mass), according to the manufacturer's instructions. IgE and B cell-activating factor (BAFF) levels were analyzed with the mouse IgE ELISA Set (BD Biosciences) and BAFF Quantikine ELISA (R&D

Systems, Minneapolis, Minn), respectively, according to the manufacturer's instructions. Pneumovax-specific IgM and TNP-KLH-specific IgM and IgG were levels quantified in serum after immunization by using ELISA, as previously described.³²

Histologic analysis

Tissue samples were collected at the time of 28 weeks and processed as previously described.²⁹ In addition, Fezf2/Fez1 expression was analyzed by using immunohistochemistry (F441; IBL America, Minneapolis, Minn). Arbitrary skin infiltration scores were calculated, scoring the following manifestations from 0 to 4 (where 0 is absent and 4 is severe): abnormalities of keratinocytes, immune cell infiltration, alterations of the epidermis, and presence of cutaneous abscesses.

***In vitro* T-cell proliferation**

For T-cell proliferation assays, 5×10^5 spleen cells were labeled with Cell-Trace Violet or FarRed cell proliferation kits (Thermo Fisher), according to the manufacturer's instructions. Labeled cells were stimulated with anti-mouse CD3e antibody (1 mg/mL; BD PharMingen), IL-2 (100 U), phorbol 12-myristate 13-acetate plus ionomycin (50 ng/ml and 1 mg/mL, respectively; Calbiochem, San Diego, Calif), and concanavalin A (2.5 µg/mL; Sigma, St Louis, Mo) and cultured in RPMI medium supplemented with 10% FBS, 1% penicillin/streptomycin, 1% glutamine, and 50 µmol/L β-mercaptoethanol (Gibco). Cells were analyzed after 3 days by using flow cytometry. Proliferation was expressed as the frequency of cells that diluted the cell proliferation dyes.

TCR spectratyping

cDNA was amplified by using constant and variable primers detailed in Table E1 in this article's Online Repository at www.jacionline.org. FAM-labeled products were analyzed by using capillary electrophoresis.

***In vivo* immunizations**

Four months after GT, mice were intraperitoneally injected with 115 µg of Pneumovax vaccine (Sanofi Pasteur, Swiftwater, Pa). Serum samples were collected weekly for 3 weeks. For TNP-KLH challenge, mice were injected intravenously with 100 µg of TNP-KLH (Biosearch Technologies, Novato, Calif). Three weeks later, animals were injected intraperitoneally with 100 µg of TNP-KLH to boost the immune response. Antigen-specific IgM and IgG antibodies were evaluated in serum by means of ELISA, as previously described.³²

Autoantibody assays

Anti-double-strand DNA antibodies were evaluated by means of ELISA, as previously described.³² Screening for a broad panel of IgM and IgG auto-antibodies was performed with autoantibody arrays (UT Southwestern Medical Center, Genomic and Microarray Core Facility, Dallas, Tex).³³

Statistical analysis

Statistical analyses were performed with GraphPad Prism software (GraphPad Software, La Jolla, Calif) by using nonparametric 1-way ANOVA with the Dunn posttest, Spearman correlation, and the nonparametric combination test. A P value of less than .05 was considered significant. Further details on significance levels are provided in figure legends.

RESULTS

GT improves peripheral B- and T-cell counts in mice with OS

Mice with OS were lethally irradiated and transplanted with Lin⁻ cells that were previously transduced with LV 2.6kbUCOERAG2co or 2.2kbUCOE-RAG2co (GT mice) to study the efficacy of GT.^{26,28} Additional mice were treated with untransduced WT or OS Lin⁻ cells as positive (BMT WT mice) and negative (BMT OS mice) controls, respectively. Starting at 6 weeks after treatment, we observed the appearance of B lymphocytes in the peripheral blood of GT mice with both vectors in marked contrast to BMT OS mice, in which this subset was virtually absent, as expected (Fig 1, A). B-cell absolute counts increased over time for 13 weeks after GT and then remained stable up to the time of 28 weeks, although at levels significantly lower than those in the BMT WT control group. After GT, we also observed an improvement in T lymphocytes, which were present in low counts in BMT OS mice (Fig 1, A and B). Moreover, the CD4⁺/CD8⁺ T-cell ratio, which is often inverted in BMT OS mice, returned to normal levels after treatment (Fig 1, C). Nonetheless, leukopenia was not fully resolved by using GT (Fig 1, D), demonstrating a partial immune reconstitution.

Overcoming the B-cell differentiation block

Mice were euthanized 7 months after treatment, and tissues were analyzed to assess immune reconstitution. Full donor chimerism (>85%, data not shown) was established in the BM, spleen, and thymus.

BM was analyzed to study B-cell development because mice with OS present a block in the initial B-cell differentiation steps due to very low levels of RAG2 activity in precursors.¹¹ GT mice showed a reduction of early B-cell precursors with the appearance of recirculating mature B cells in the BM (Fig 2, A). Although GT mice displayed a statistically significant increase in mature B-cell counts compared with BMT OS mice, only a few of them exhibited counts comparable with those in BMT WT mice (Fig 2, B). The results obtained were in accordance with the VCN in BM of GT mice (VCN, 1.0 ± 1.0 for 2.6kbUCOE-RAG2co GT mice; VCN, 0.3 ± 0.2 for 2.2kbUCOE-RAG2co GT mice), and a statistically significant correlation between VCN and mature recirculating B cell counts was found (see Fig E1, A, in this article's Online Repository at www.jacionline.org).

In the spleen, absolute counts were normal in some GT mice but low or similar to counts in BMT OS mice in others (Fig 2, C). Consistently, variability in the splenic B-cell counts and vector-driven RAG2 expression positively correlated with VCN, underscoring the importance of sufficient RAG2 expression for proper immune reconstitution (VCN in spleen, 1.8 ± 1.0 and 1.4 ± 0.2 for GT 2.6kbUCOE-RAG2co and GT 2.2kbUCOE-RAG2co, respectively; see Fig E1, A and B). In particular, BMT OS mice had few immature

transitional cells, whereas GT allowed normal maturation of marginal zone and follicular B cells with a relative increase in the frequency of marginal zone cells (Fig 2, D, and see Fig E1, C), likely because of the lymphopenic environment.³⁴

To evaluate the functionality of B cells after therapy, we measured immunoglobulin levels in the serum of our cohorts of mice at the time of 28 weeks. We achieved normalization in IgM, IgA, and IgG production, thus indicating that even low B-cell numbers were able to produce adequate immunoglobulin levels. Furthermore, IgE levels, which were usually increased in mice with OS,^{27,35} returned to low levels of BMT WT mice (Fig 2, E).

Amelioration of thymic architecture and output

GT was able to partially restore thymic structure and function. Histology and immunostaining revealed restoration of corticomedullary demarcation. The medulla area was variable in GT mice and consistent with VCN retrieved in thymocytes (Fig 3, A). GT mice, in particular those treated with LV 2.6kbUCOERAG2co, showed a marked improvement in the medulla/cortex ratio, even if they did not reach the levels of BMT WT control mice (Fig 3, B). Furthermore, thymic recovery was found to significantly correlate with VCN (Fig 3, C). Because defects in central tolerance have been described in patients with OS and in mouse counterparts,^{27,36} we evaluated expression of autoimmune regulator (AIRE), the master gene regulator of the promiscuous expression of tissue-restricted antigens in the thymus.³⁷ AIRE⁺ cells were dramatically reduced in BMT OS control mice, as expected, and were increased only in the minority of GT mice, suggesting incomplete maturation of medullary thymic epithelial cells, particularly in GT mice with lower VCN (Fig 3, D, and see Fig E2 in this article's Online Repository at www.jacionline.org). We also measured the expression of Fezf2, which was recently identified as a key regulator of AIRE-independent tissue-restricted antigen gene expression.³⁸ Similar to AIRE, the low frequency of Fezf2⁺ cells was corrected partly in the group treated with LV 2.6kbUCOE-RAG2co (Fig 3, E, and see Fig E2, A and B). Finally, we investigated the thymocyte compartment. GT mice showed improved thymic cellularity (Fig 3, F), with a high variability explained by strong differences in human RAG2 expression (VCN, 2.1 6 1.9 and 1.7 ± 1.7 for GT 2.6kbUCOE-RAG2co and GT 2.2kbUCOERAG2co mice, respectively; Fig 3, G, and see Fig E1, D). CD4⁻CD8⁻ double-negative precursors were indeed predominant in the poorly immune reconstituted thymi of BMT OS mice. After GT, this subpopulation diminished dramatically with an expansion of CD4⁺CD8⁺ double-positive cells, reestablishing a subset distribution similar to that of BMT WT thymus (Fig 3, H). On the other hand, mature single-positive CD4⁺CD8⁻ and CD8⁺CD4⁻ T cells presented a similar frequency in all groups analyzed.

Recovery of T-cell phenotype and function

We examined T-cell numbers and immunophenotypes in the spleen 7 months after treatment. Similar to B lymphocytes, GT provided a statistically significant increase in T-cell counts, even though they remained notably lower than in BMT WT mice (Fig 4, A, and see Fig E1, D). Moreover, we detected the reestablishment of a correct CD4⁺/CD8⁺ T-cell ratio (Fig 4, B) similar to peripheral blood. Detailed investigation of T cells in GT mice revealed the appearance of naive CD4⁺ and CD8⁺ lymphocytes. Indeed, in mice with OS, the vast

majority of T cells showed an activated phenotype (Fig 4, C). Again, the frequency and counts of naive T cells after therapy remained lower compared with those in WT-transplanted control mice. Hence we moved to analyze T-cell functionality *in vitro*. Spleen cell proliferation was induced with different combinations of TCR-dependent (α CD3 and IL-2) or TCR-independent (phorbol 12-myristate 13-acetate plus ionomycin and concanavalin A) stimuli. Although CD8⁺ T lymphocytes from BMT OS mice were unresponsive, GT mice behaved similarly to BMT WT control mice in response to all stimuli (Fig 4, D). The same results were obtained in CD4⁺ T cells (see Fig E3 in this article's Online Repository at www.jacionline.org).

Furthermore, we analyzed TCR V β repertoire diversity using fragment length analysis (spectratyping) to assess TCR rearrangements as an indirect measure of the restoration of RAG2 activity. As expected, BMT OS mice presented a skewed oligoclonal TCR repertoire. GT mice with an adequate reconstitution level revealed a predominantly polyclonal spectratype superimposable to those of BMT WT samples (Fig 4, E, GT3 mouse). Conversely, GT mice, in which the VCN was low and immune reconstitution was poor, showed an oligoclonal repertoire comparable with that in BMT OS mice (GT4 mouse with low VCN and GT5 mouse with intermediate VCN; Fig 4, E).

Efficient response to *in vivo* challenges

To understand whether B and T lymphocytes were functional *in vivo*, 3 months after transplantation, we challenged GT mice with antigens to induce T-dependent or T-independent immune responses. The first group was injected intraperitoneally with the P23 Pneumovax vaccine, which elicits a T-independent B-cell response. Three weeks after vaccination, we quantified antigen-specific IgM production, revealing the incapacity of BMT OS mice to mount an immune response. On the contrary, B cells of GT mice generated a P23-specific IgM response superimposable to that of WT mice undergoing transplantation (Fig 5, A). The variability of the immune response to Pneumovax depended on the extent of immune reconstitution because it correlated statistically with B-cell counts in the spleen (Fig 5, B). The second group of mice was challenged with TNP-KLH antigens that induce a T-dependent B-cell response to evaluate the crosstalk between T and B cells. Three weeks after injection, antigen-specific IgM production was absent in BMT OS mice but properly recovered in GT mice (Fig 5, C). A second boost dose was administered to previously immunized mice to study the T-dependent immunoglobulin class-switching. One week later, antigen-specific IgG levels were measured in the serum of treated mice. As predicted, IgG levels were undetectable in sera from BMT OS mice, whereas GT-treated mice presented an IgG stimulation index comparable with that of BMT WT control mice (Fig 5, D). Similar to Pneumovax immunization, the extent of the immune response to TNP-KLH correlated with the absolute counts of B and T cells in the spleen (Fig 5, E).

Partial improvement of autoimmune manifestations

Inflammation and autoimmune-like manifestations are peculiar in the setting of OS, and therefore we investigated factors associated with autoimmunity. We examined BAFF, which is required for B-cell survival and homeostasis and linked to the emergence of autoimmunity when overproduced.³⁹ BAFF levels were increased in the sera of BMT OS mice, probably

because of the lack of its target B lymphocytes. GT mice exhibited a reduction in serum BAFF levels, although statistically greater than those in BMT WT mice (Fig 6, A). Circulating anti–double-stranded DNA autoantibodies were present in 22% of GT mice and absent in BMT OS mice, likely because of the complete absence of B cells after total-body irradiation (Fig 6, B). Furthermore, to extend the analysis to a broader panel of autoantigens, we tested a high-throughput autoantigen microarray platform containing 123 different autoantigens. We did not observe any significant changes in IgM and IgG autoantibody production in GT mice compared with BMT WT mice (Fig 6, C). Conversely, positivity for a broad panel of autoantigens was detected in sera obtained from untreated tested mice with OS (Fig 6, D, and see Table E2 in this article’s Online Repository at www.jacionline.org).

A typical OS hallmark is skin erythroderma caused by infiltration of CD3⁺ T lymphocytes and eosinophils and, consequently, dermal inflammation.²⁷ Alteration of the keratin layer, immune cell infiltration, thickness of the epidermis, and presence of cutaneous abscesses were graded to calculate an arbitrary inflammatory skin score (the higher, the more severe). At the time of 28 weeks, BMT OS mice displayed severe skin manifestations. GT mice showed mitigation of the symptoms, although strong variability was observed because some mice exhibited skin alterations and immune infiltration, whereas others had a completely normal skin phenotype (Fig 7, A and B). These findings were explained by the variability in immune reconstitution achieved with GT. Because VCN could not be calculated in the skin, we correlated the infiltration score with B- and T-cell counts in the blood at the time of 28 weeks as a measure of posttreatment reconstitution and observed a statistically significant inverse correlation (Fig 7, C), indicating that the mice in which the skin inflammation score was greater were those in which T- and B-cell reconstitution was lower.

Overall, our findings indicate a substantial, although incomplete, correction of the Omenn phenotype, as shown in Table I.

DISCUSSION

Mutations in *RAG* genes are responsible for a broad spectrum of clinical manifestations. Allogeneic HSCT is the standard of care, ideally performed before onset of life-threatening complications and organ damage, but its overall outcome remains unsatisfactory and can be recommended only when a matched donor is available.^{12,17,18,40} In this scenario GT might represent a powerful alternative approach, as demonstrated by encouraging results obtained in recent clinical primary immunodeficiency (PID) trials.⁴¹ Preclinical studies in the *Rag2*^{-/-} model indicated UCOE as the most promising promoter to drive expression of human *RAG2* transgene,²⁶ and on this basis, we tested whether this approach could rescue defects with residual RAG activity. OS represents a paradigmatic model because of severe inflammation and dysregulated immune environment. We exploited the *Rag2*^{R229Q/R229Q} mouse, faithfully recapitulating human OS disease. Indeed, *Rag2*^{R229Q/R229Q} mice have an expansion of oligoclonal autoreactive T cells infiltrating organs, including the skin and gut, and a virtual absence of circulating B cells in the presence of increased serum IgE levels.^{42,43} Dramatic alterations in thymic architecture with consequent impairment in negative selection of thymocytes were reported both in mice and patients with OS.⁴⁴ Here we used the 2.6kbUCOE-RAG2co vector tested in the *Rag2*^{-/-} murine model,²⁶ and in parallel, we tested

the shortened 2.2-kb version of UCOE.²⁸ GT follow-up lasted 28 weeks, during which a minor fraction of treated mice died because of lack of immune reconstitution and disease progression similar to BMT OS mice (see Fig E4 and Table E3 in this article's Online Repository at www.jacionline.org). Of note, a thymic mass was observed at autopsy in 1 of 35 GT-treated mice. Immunohistochemical analysis of the thymus revealed a lymphoproliferative expansion of CD3⁺ cells in the absence of peripheral CD3 expansion.

B-cell development in mice with OS is arrested in part at the B-cell progenitor stage, with consequent reduction in splenic B cells and relative expansion of immature transitional B cells. In the BM partial B-cell subset redistribution was observed in both GT groups. In the periphery splenic B-cell counts were lower than those in BMT WT control mice, although increased compared with those in BMT OS mice. Importantly, GT induced a marked reduction in the immature transitional B-cell fraction and relative expansion of marginal zone B cells that in a lymphopenic environment might indicate increased exposure to blood-borne antigens.^{34,45} In peripheral blood transduced B cells appeared and increased in number over time, remaining stable up to 7 months, although at lower frequencies and counts than in the BMT WT group. Nonetheless, these results are in line with data reported in the *Rag2* knockout model.²⁶ The 2.2kbUCOE vector showed slower B-cell reconstitution but reached counts comparable with the 2.6-kb LV at the latest time point. However, analysis of serum immunoglobulin production indicated a normalization of IgM sub-type, whereas IgG levels were more variable and increased compared with those in the BMT OS group. Serum IgE levels were reduced in both GT groups and reached levels similar to those of BMT WT mice. Of note, serum BAFF levels were increased in BMT OS mice, as well as in mice and patients with OS,^{9,11} and diminished in the majority of GT-treated mice, although not reaching BMT WT serum levels. However, IgM and IgG serum autoantibody profiles did not reveal any gross alterations in GT-treated mice. *In vivo* challenges demonstrated that GT mice responded to T cell-dependent and T cell-independent antigens by producing antigen-specific antibodies, indicating that B cells, although reduced in numbers, are able to mount a proper response.

Analysis of VCN in both BM and spleens indicated a significant correlation between B-cell recovery and expression of the transgene. However, VCN values of greater than 2 did not always correlate with faster B-cell reconstitution and higher peripheral B-cell counts, suggesting that tightly regulated *Rag2* expression might be required to obtain an adequate B-cell development. To overcome this hurdle, gene editing strategies mediated by various nucleases are currently in early-phase development to achieve precise genetic correction and avoid unregulated gene expression.⁴⁶ Furthermore, the human *RAG2* expressed by UCOE vectors might prevent complete immune reconstitution in GT mice. Indeed, species-specific differences might hamper the ability of human *RAG2* to bind the murine *RAG1* zinc finger regions and form the fully functional *RAG1*-*RAG2* recombinase complex, thus limiting the complex enzymatic activity.⁴⁷

Overall, data observed in this preclinical model show partial reconstitution of the B-cell compartment, similar to that seen in patients with SCID, who are functionally agammaglobulinemic and require intravenous immunoglobulin replacement therapy because

of poor B-cell reconstitution despite successful T-cell reconstitution after HSCT and pretransplantation conditioning.^{48,49}

In contrast to B cells, transduced T-cell progenitors show a higher selective advantage. A detailed analysis of thymic epithelium indicates a substantial improvement in corticomedullary demarcation and maturation of the medullary thymic epithelial cell compartment with expression of AIRE and Fezf2, 2 independent factors controlling tissue-restricted antigen expression and governing central tolerance mechanisms, which are defective in mice with OS, leading to autoreactive T-cell survival.^{27,42} Of note, VCN values indicate a positive correlation with formation of the medulla compartment and RAG2 expression. Consistently, gene-corrected thymocytes increased in number, overcoming the block at the double-negative 3 stage and expanding the double-positive and single-positive thymocyte populations and demonstrating the occurrence of normal V(D)J recombination. The analysis of VCN in the thymus showed higher values than those detected in total BM, suggesting the existence of a selective advantage for corrected T-lymphocyte precursors (see Fig E5, A and C, in this article's Online Repository at www.jacionline.org). However, comparable results were obtained in Rag2^{-/-} mice, in which a partial correction of the thymic defect was sufficient to substantially improve lymphopenia, the peripheral T phenotype, and compartmentalization of thymic epithelium.²⁶ These findings suggest that additional pharmacologic pretreatments might be needed to improve thymic reconstitution, in particular in the case of OS.²⁹ In this regard it is important to emphasize that the Rag2^{-/-} mouse does not present inflammatory and autoimmune features typical of OS that can further affect thymic microenvironment. Important alterations in central tolerance have been described in the murine OS model and in patients, indicating that both the correction of thymic epithelial function and the immunologic reconstitution are critical to obtain a significant improvement in peripheral immunopathology. Indeed, lower survival and a higher rate of clinical problems after transplantation have been observed in patients with SCID treated after 3.5 months of age, when the thymus is more severely affected.¹⁴

Despite lower absolute counts of circulating and splenic T cells, the CD4/CD8 T-cell ratio normalized in the periphery. Importantly, T cells characterized by an effector phenotype in BMT OS mice showed a redistribution of subpopulations with the appearance of naive CD4⁺ and CD8⁺ T cells. Immunoscope analysis revealed a V β polyclonal distribution that correlated with VCN. *In vitro* T-cell proliferation confirmed the functionality of gene-corrected T cells, which was similar to that of cells isolated from the spleens of BMT WT mice.

Finally, GT decreased the severity of skin damage, the hallmark of OS. Epidermal and dermal infiltration were reduced in GT mice, and the improvement was more evident in mice with higher B- and T-cell counts. These findings are clinically relevant because they provide additional proof that T cells with sufficient transgene expression are properly corrected and no longer autoreactive. Our results offer hope for a prospective evaluation of GT intervention in other PIDs characterized by autoimmunity and inflammation, particularly in immune defects caused by hypomorphic mutations in genes of the V(D)J recombination process. For many of these PIDs, several preclinical studies using improved viral vectors are ongoing, with the ultimate goal to determine their clinical applicability.⁵⁰⁻⁵³ These

preclinical studies will allow us to understand to what extent inflammation and competition between endogenous uncorrected and corrected progenitors affect immune reconstitution and will also clarify the effects of deregulated protein expression on the immune system.

To overcome problems related to the ectopic and nonphysio-logic expression of therapeutic genes,^{54–56} genome editing strategies in hematopoietic stem cells are now emerging. However, gene addition currently remains a valid option for several genetic disorders, as a result of technical advances in vector production, improved transduction, and maintenance of hematopoietic stem cell stemness and fitness.^{50,57} In this regard the availability of *in vivo* models, such as our *Rag2* hypomorphic mutant, represents a valuable tool for the systematic study of efficacy and safety of novel medical interventions.

In conclusion, our findings provide the rationale to further develop GT and editing approaches, even in the presence of inflammation and autoimmunity.

Supplementary Material

Refer to Web version on PubMed Central for supplementary material.

Acknowledgments

Supported by the Italian Telethon foundation (Telethon Core TGT E2 Grant to A.V.); by the European Commission's 5th, 6th, and 7th and Horizon 2020 Framework Programs (contracts QLK3-CT-2001–00427-INHERINET, LSHB-CT-2004–005242-CONCERT, grant agreement 261387 CELL-PID to A.V. and grant 666908-SCIDNET to A.V.); and by The Netherlands Health Research and Development Organization ZonMw, Translational Gene Therapy Program (project 43100016 to G.W.) and by Italian Ministry of Health (grant GR-2011–02349759 to B.C.).

Disclosure of potential conflict of interest: L. D. Notarangelo is Editor of *Frontiers in Immunology*, Associate Editor for the *Journal of Clinical Immunology*, and Associate Editor for *Clinical Immunology*; is employed by the National Institutes of Health and the Department of Health and Human Services; and has received royalties from UpTo-Date. G. Wagemaker has received grants and travel support from The Netherlands Organization for Health Research ZonMw and the European Commission. A. Villa has received a grant from the European Commission. The rest of the authors declare that they have no relevant conflict of interest.

We thank Michael N. Antoniou (Department of Medical and Molecular Genetics, King's College London, London, United Kingdom), who provided the short UCOE element. We thank Federica Cugnata (University Centre for Statistics in the Biomedical Sciences, CUSSB, Universit a Vita-Salute San Raffaele, Milan, Italy) for assistance in the statistical analyses.

Abbreviations used

AIRE	Autoimmune regulator
BAFF	B cell–activating factor
BM	Bone marrow
GT	Gene therapy
HSCT	Hematopoietic stem cell transplantation
Lin[−]	Lineage negative
LV	Lentiviral vector

OS	Omenn syndrome
PID	Primary immunodeficiency
RAG	Recombination-activating gene
SCID	Severe combined immunodeficiency
TCR	T-cell receptor
UCOE	Ubiquitous chromatin opening element
VCN	Vector copy number/genome
WT	Wild-type

REFERENCES

1. Notarangelo LD, Kim M-S, Walter JE, Lee YN. Human RAG mutations: biochemistry and clinical implications. *Nat Rev Immunol* 2016;16:234–46. [PubMed: 26996199]
2. Abolhassani H, Wang N, Aghamohammadi A, Rezaei N, Lee YN, Frugoni F, et al. A hypomorphic recombination-activating gene 1 (RAG1) mutation resulting in a phenotype resembling common variable immunodeficiency. *J Allergy Clin Immunol* 2014;134:1375–80. [PubMed: 24996264]
3. Kato T, Crestani E, Kamae C, Honma K, Yokosuka T, Ikegawa T, et al. RAG1 deficiency may present clinically as selective IgA deficiency. *J Clin Immunol* 2015;35:280–8. [PubMed: 25739914]
4. Buchbinder D, Baker R, Lee YN, Ravell J, Zhang Y, McElwee J, et al. Identification of patients with RAG mutations previously diagnosed with common variable immunodeficiency disorders. *J Clin Immunol* 2015;35:119–24. [PubMed: 25516070]
5. Cifaldi C, Angelino G, Chiriaco M, Di Cesare S, Claps A, Serafinelli J, et al. Late-onset combined immune-deficiency due to LIGIV mutations in a 12 years old patient. *Pediatr Allergy Immunol* 2017;28:203–6. [PubMed: 27893162]
6. Omenn GS. Familial reticuloendotheliosis with eosinophilia. *N Engl J Med* 1965; 273:427–32. [PubMed: 14328107]
7. Villa A, Santagata S, Bozzi F, Giliani S, Frattini A, Imberti L, et al. Partial V(D)J recombination activity leads to omenn syndrome. *Cell* 1998;93:885–96. [PubMed: 9630231]
8. Corneo B, Moshous D, Günçör T, Wulffraat N, Philippet P, Le Deist F, et al. Identical mutations in RAG1 or RAG2 genes leading to defective V(D)J recombinase activity can cause either T-B-severe combined immune deficiency or Omenn syndrome. *Blood* 2001;97:2772–6. [PubMed: 11313270]
9. Walter JE, Rucci F, Patrizi L, Recher M, Regenass S, Paganini T, et al. Expansion of immunoglobulin-secreting cells and defects in B cell tolerance in Rag-dependent immunodeficiency. *J Exp Med* 2010;207:1541–54. [PubMed: 20547827]
10. Walter JE, Rosen LB, Csomos K, Rosenberg JM, Mathew D, Keszei M, et al. Broad-spectrum antibodies against self-antigens and cytokines in RAG deficiency. *J Clin Invest* 2015;125:4135–48. [PubMed: 26457731]
11. Cassani B, Poliani PL, Marrella V, Schena F, Sauer AV, Ravanini M, et al. Homeostatic expansion of autoreactive immunoglobulin-secreting cells in the Rag2 mouse model of Omenn syndrome. *J Exp Med* 2010;207:1525–40. [PubMed: 20547828]
12. Pai S-Y, Logan BR, Griffith LM, Buckley RH, Parrott RE, Dvorak CC, et al. Transplantation outcomes for severe combined immunodeficiency, 2000–2009. *N Engl J Med* 2014;371:434–46. [PubMed: 25075835]
13. Myers LA, Patel DD, Puck JM, Buckley RH. Hematopoietic stem cell transplantation for severe combined immunodeficiency in the neonatal period leads to superior thymic output and improved survival. *Blood* 2002;99:872–8. [PubMed: 11806989]

14. Railey MD, Lokhnygina Y, Buckley RH. Long-term clinical outcome of patients with severe combined immunodeficiency who received related donor bone marrow transplants without pretransplant chemotherapy or post-transplant GVHD prophylaxis. *J Pediatr* 2009;155:834–40.e1. [PubMed: 19818451]
15. Gennery AR, Slatter MA, Grandin L, Taupin P, Cant AJ, Veys P, et al. Transplantation of hematopoietic stem cells and long-term survival for primary immunodeficiencies in Europe: entering a new century, do we do better? *J Allergy Clin Immunol* 2010;126:602–10, e1–11. [PubMed: 20673987]
16. Buckley RH, Win CM, Moser BK, Parrott RE, Sajaroff E, Sarzotti-Kelsoe M. Post-transplantation B cell function in different molecular types of SCID. *J Clin Immunol* 2013;33:96–110. [PubMed: 23001410]
17. Heimall J, Puck J, Buckley R, Fleisher TA, Gennery AR, Neven B, et al. Current knowledge and priorities for future research in late effects after hematopoietic stem cell transplantation (HCT) for severe combined immunodeficiency patients: a consensus statement from the Second Pediatric Blood and Marrow Transplant Consortium. *Biol Blood Marrow Transplant* 2017;23:379–87. [PubMed: 28068510]
18. Schuetz C, Neven B, Dvorak CC, Leroy S, Ege MJ, Pannicke U, et al. SCID patients with ARTEMIS vs RAG deficiencies following HCT: Increased risk of late toxicity in ARTEMIS-deficient SCID. *Blood* 2014;123:281–9. [PubMed: 24144642]
19. Cavazzana M, Six E, Lagresle-Peyrou C, André-Schmutz I, Hacein-Bey-Abina S. Gene therapy for X-linked severe combined immunodeficiency: where do we stand? *Hum Gene Ther* 2016;27:108–16. [PubMed: 26790362]
20. De Ravin SS, Wu X, Moir S, Anaya-O'Brien S, Kwatema N, Littel P, et al. Lentiviral hematopoietic stem cell gene therapy for X-linked severe combined immunodeficiency. *Sci Transl Med* 2016;8:335ra57.
21. Aiuti A, Cattaneo F, Galimberti S, Benninghoff U, Cassani B, Callegaro L, et al. Gene therapy for immunodeficiency due to adenosine deaminase deficiency. *N Engl J Med* 2009;360:447–58. [PubMed: 19179314]
22. Candotti F, Shaw KL, Muul L, Carbonaro D, Sokolic R, Choi C, et al. Gene therapy for adenosine deaminase-deficient severe combined immune deficiency: clinical comparison of retroviral vectors and treatment plans. *Blood* 2012;120: 3635–46. [PubMed: 22968453]
23. Van Til NP, Sarwari R, Visser TP, Hauer J, Lagresle-Peyrou C, Van Der Velden G, et al. Recombination-activating gene 1 (Rag1)-deficient mice with severe combined immunodeficiency treated with lentiviral gene therapy demonstrate autoimmune Omenn-like syndrome. *J Allergy Clin Immunol* 2014;133:1116–23. [PubMed: 24332219]
24. Pike-Overzet K, Rodijk M, Ng Y-Y, Baert MRM, Lagresle-Peyrou C, Schambach A, et al. Correction of murine Rag1 deficiency by self-inactivating lentiviral vector-mediated gene transfer. *Leukemia* 2011;25:1471–83. [PubMed: 21617701]
25. Yates F, Malassis-Séris M, Stockholm D, Bouneaud C, Larousserie F, Noguez-Hellin P, et al. Gene therapy of RAG-2^{-/-} mice: sustained correction of the immunodeficiency. *Blood* 2002;100:3942–9. [PubMed: 12393742]
26. van Til NP, de Boer H, Mashamba N, Wabik A, Huston M, Visser TP, et al. Correction of murine Rag2 severe combined immunodeficiency by lentiviral gene therapy using a codon-optimized RAG2 therapeutic transgene. *Mol Ther* 2012;20:1968–80. [PubMed: 22692499]
27. Marrella V, Poliani PL, Casati A, Rucci F, Frascoli L, Gougeon ML, et al. A hypomorphic R229Q Rag2 mouse mutant recapitulates human Omenn syndrome. *J Clin Invest* 2007;117:1260–9. [PubMed: 17476358]
28. Knight S, Zhang F, Mueller-Kuller U, Bokhoven M, Gupta A, Broughton T, et al. Safer, silencing-resistant lentiviral vectors: optimization of the ubiquitous chromatin-opening element through elimination of aberrant splicing. *J Virol* 2012;86:9088–95. [PubMed: 22696657]
29. Marrella V, Poliani PL, Fontana E, Casati A, Maina V, Cassani B, et al. Anti-CD3e mAb improves thymic architecture and prevents autoimmune manifestations in a mouse model of Omenn syndrome: therapeutic implications. *Blood* 2012;120:1005–14. [PubMed: 22723555]

30. Chiriaco M, Farinelli G, Capo V, Zonari E, Scaramuzza S, Di Matteo G, et al. Dual-regulated lentiviral vector for gene therapy of X-linked chronic granulomatosis. *Mol Ther* 2014;22:1472–83. [PubMed: 24869932]
31. Marangoni F, Bosticardo M, Charrier S, Draghici E, Locci M, Scaramuzza S, et al. Evidence for long-term efficacy and safety of gene therapy for Wiskott-Aldrich syndrome in preclinical models. *Mol Ther* 2009;17:1073–82. [PubMed: 19259069]
32. Bosticardo M, Draghici E, Schena F, Sauer AV, Fontana E, Castiello MC, et al. Lentiviral-mediated gene therapy leads to improvement of B-cell functionality in a murine model of Wiskott-Aldrich syndrome. *J Allergy Clin Immunol* 2011;127:1376–84.e5. [PubMed: 21531013]
33. Li QZ, Zhou J, Wandstrat AE, Carr-Johnson F, Branch V, Karp DR, et al. Protein array autoantibody profiles for insights into systemic lupus erythematosus and incomplete lupus syndromes. *Clin Exp Immunol* 2007;147:60–70. [PubMed: 17177964]
34. Hao Z, Rajewsky K. Homeostasis of peripheral B cells in the absence of B cell influx from the bone marrow. *J Exp Med* 2001;194:1151–64. [PubMed: 11602643]
35. Rigoni R, Fontana E, Guglielmetti S, Fosso B, D'Erchia AM, Maina V, et al. Intestinal microbiota sustains inflammation and autoimmunity induced by hypomorphic RAG defects. *J Exp Med* 2016;213:355–75. [PubMed: 26926994]
36. Cavadini P, Vermi W, Facchetti F, Fontana S, Nagafuchi S, Mazzolari E, et al. AIRE deficiency in thymus of 2 patients with Omenn syndrome. *J Clin Invest* 2005;115:728–32. [PubMed: 15696198]
37. Abramson J, Husebye ES. Autoimmune regulator and self-tolerance—molecular and clinical aspects. *Immunol Rev* 2016;271:127–40. [PubMed: 27088911]
38. Takaba H, Morishita Y, Tomofuji Y, Danks L, Nitta T, Komatsu N, et al. Fezf2 orchestrates a thymic program of self-antigen expression for immune tolerance. *Cell* 2015;163:975–87. [PubMed: 26544942]
39. Cancro MP. Signalling crosstalk in B cells: managing worth and need. *Nat Rev Immunol* 2009;9:657–61. [PubMed: 19704418]
40. Neven B, Leroy S, Decaluwe H, Le Deist F, Picard C, Moshous D, et al. Long-term outcome after hematopoietic stem cell transplantation of a single-center cohort of 90 patients with severe combined immunodeficiency. *Blood* 2009; 113:4114–24. [PubMed: 19168787]
41. Booth C, Gaspar HB, Thrasher AJ. Treating immunodeficiency through HSC gene therapy. *Trends Mol Med* 2016;22:317–27. [PubMed: 26993219]
42. Marrella V, Poliani PL, Notarangelo LD, Villa A. Rag defects and thymic stroma: lessons from animal models. *Front Immunol* 2014;5:259. [PubMed: 25076946]
43. Maina V, Marrella V, Mantero S, Cassani B, Fontana E, Anselmo A, et al. Hypomorphic mutation in the RAG2 gene affects dendritic cell distribution and migration. *J Leukoc Biol* 2013;94:1221–30. [PubMed: 24052573]
44. Poliani PL, Facchetti F, Ravanini M, Gennery AR, Villa A, Roifman CM, et al. Early defects in human T-cell development severely affect distribution and maturation of thymic stromal cells: possible implications for the pathophysiology of Omenn syndrome. *Blood* 2009;114:105–8. [PubMed: 19414857]
45. Srivastava B, Quinn WJ, Hazard K, Erikson J, Allman D. Characterization of marginal zone B cell precursors. *J Exp Med* 2005;202:1225–34. [PubMed: 16260487]
46. Cornu TI, Mussolino C, Cathomen T. Refining strategies to translate genome editing to the clinic. *Nat Med* 2017;23:415–23. [PubMed: 28388605]
47. Schatz DG, Swanson PC. V(D)J recombination: mechanisms of initiation. *Annu Rev Genet* 2011;45:167–202. [PubMed: 21854230]
48. Buckley RH. B-cell function in severe combined immunodeficiency after stem cell or gene therapy: a review. *J Allergy Clin Immunol* 2010;125: 790–7. [PubMed: 20371393]
49. Haddad E, Leroy S, Buckley RH. B-cell reconstitution for SCID: should a conditioning regimen be used in SCID treatment? *J Allergy Clin Immunol* 2013;131: 994–1000. [PubMed: 23465660]
50. Thrasher AJ, Williams DA. Evolving gene therapy in primary immunodeficiency. *Mol Ther* 2017;25:1132–41. [PubMed: 28366768]

51. Fischer A, Provot J, Jais J-P, Alcais A, Mahlaoui N. members of the CEREDIH French PID study group. Autoimmune and inflammatory manifestations occur frequently in patients with primary immunodeficiencies. *J Allergy Clin Immunol* 2017;140:1388–98.e8. [PubMed: 28192146]
52. Seidel MG. Autoimmune and other cytopenias in primary immunodeficiencies: pathomechanisms, novel differential diagnoses, and treatment. *Blood* 2014;124: 2337–44. [PubMed: 25163701]
53. Candotti F Advances of gene therapy for primary immunodeficiencies. *F1000Research* 2016;5:310.
54. Genovese P, Schirotti G, Escobar G, Di Tomaso T, Firrito C, Calabria A, et al. Targeted genome editing in human repopulating haematopoietic stem cells. *Nature* 2014;510:235–40. [PubMed: 24870228]
55. De Ravin SS, Li L, Wu X, Choi U, Allen C, Koontz S, et al. CRISPR-Cas9 gene repair of hematopoietic stem cells from patients with X-linked chronic granulomatous disease. *Sci Transl Med* 2017;9:eaah3480. [PubMed: 28077679]
56. Kohn DB, Kuo CY. New frontiers in the therapy of primary immunodeficiency: from gene addition to gene editing. *J Allergy Clin Immunol* 2017; 139:726–32. [PubMed: 28270364]
57. Dever DP, Porteus MH. The changing landscape of gene editing in hematopoietic stem cells: a step towards Cas9 clinical translation. *Curr Opin Hematol* 2017;24: 481–8. [PubMed: 28806273]

Key message

- LV-mediated GT improves immune dysregulation and skin infiltration in the setting of OS.

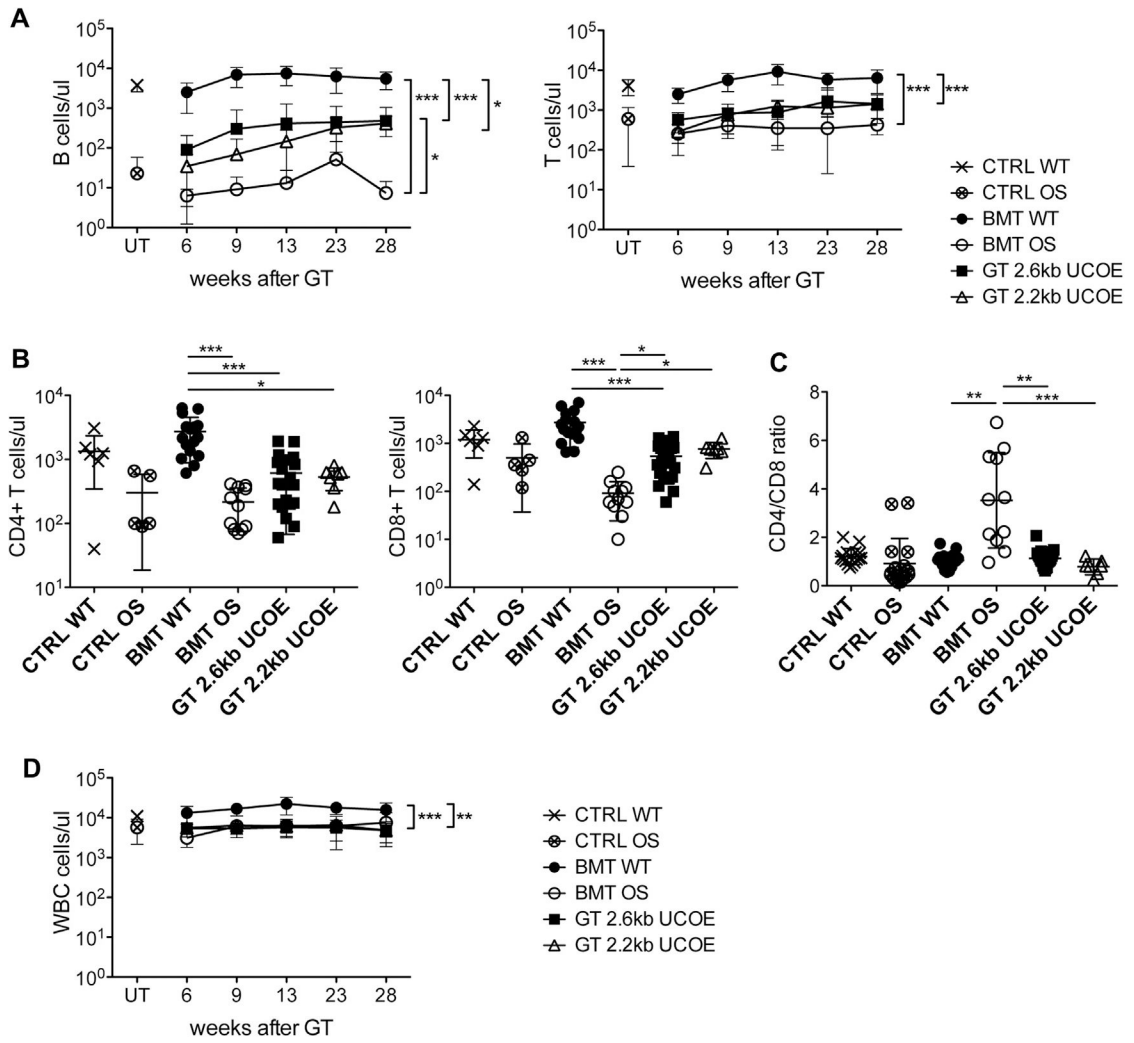


FIG 1. Peripheral blood Immune reconstitution. **A**, Absolute counts of B (*left*) and T (*right*) lymphocytes at indicated time points after treatment. CTRL WT and CTRL OS mice, n = 17; BMT WT and BMT OS mice, n = 16; GT 2.6kbUCOE mice, n = 25; GT 2.2kbUCOE mice, n = 7. **B**, Absolute counts of CD4⁺ (*left*) and CD8⁺ (*right*) T cells in peripheral blood at the time of 28 weeks in untreated (CTRL WT and CTRL OS mice) or transplanted (BMT WT, BMT OS, and GT mice) mice. **C**, Ratio between CD4⁺ and CD8⁺ T cells at the time of 28 weeks. **D**, Absolute counts of WBCs at indicated time points after treatment. CTRL WT and CTRL OS mice, n = 17; BMT WT and BMT OS mice, n = 16; GT 2.6kbUCOE mice, n = 25; GT 2.2kbUCOE mice, n = 7. All data are means ± SDs. Statistical significance was determined by using nonparametric 1-way ANOVA with the Dunn posttest, excluding untreated groups. *UT*, Untreated. **P* < .05, ***P* < .01, and ****P* < .001.

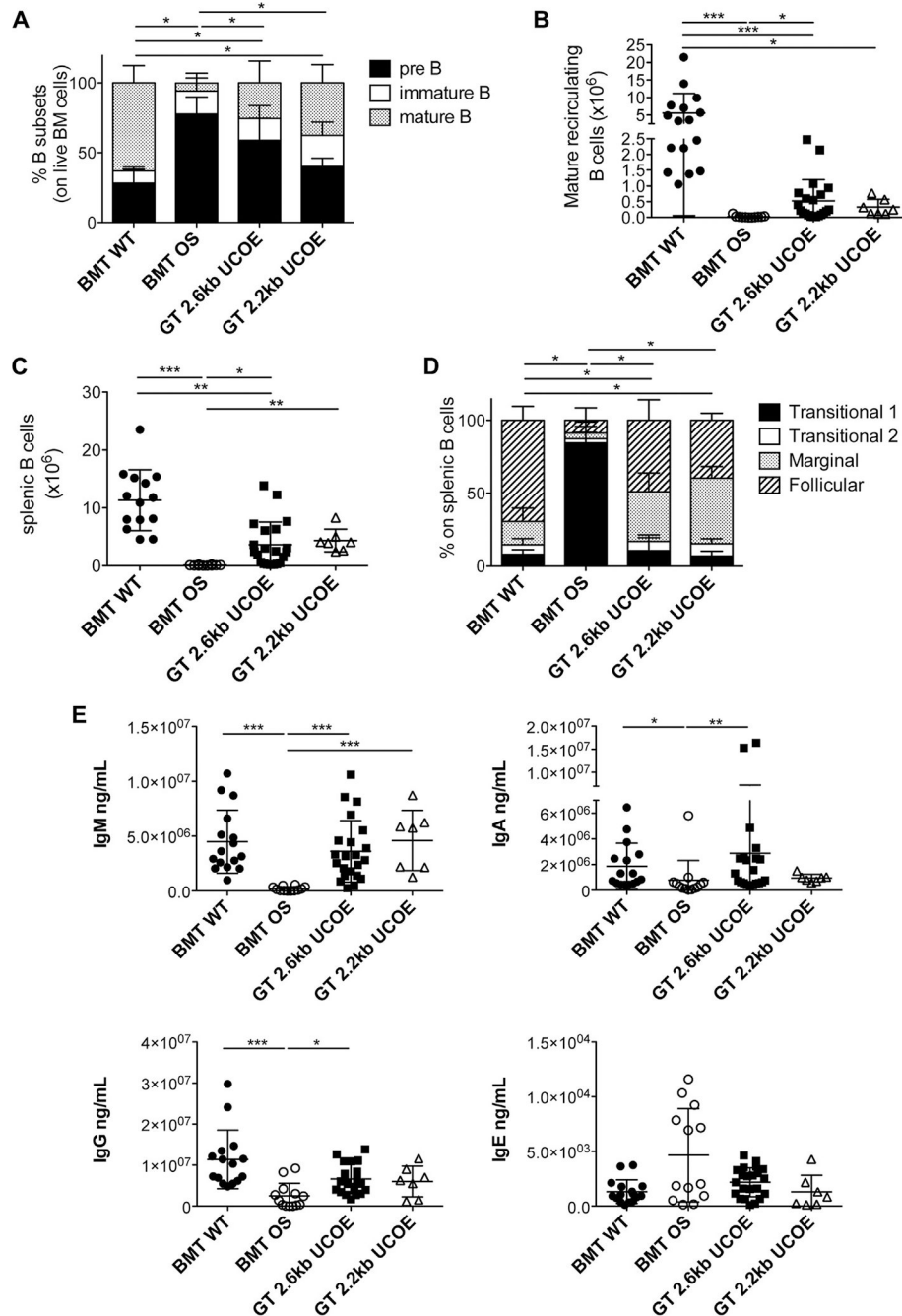


FIG 2. B-cell development and functionality. **A**, Relative frequencies of pre-B, immature, and mature recirculating B-cell populations in BM. BMT WT mice, n = 16; BMT OS mice, n = 11; GT 2.6kbUCOE mice, n = 21; GT 2.2kbUCOE mice, n = 7. **B**, Counts of mature recirculating B cells in BM. **C**, Counts of B lymphocytes in the spleen. **D**, Relative frequencies of transitional, marginal, and follicular B-cell populations in the spleen. BMT WT mice, n = 16; BMT OS mice, n = 10; GT 2.6kbUCOE mice, n = 21; GT 2.2kbUCOE mice, n = 7. **E**, IgM, IgA, IgG, and IgE levels in sera of transplanted mice at the time of 28

weeks. Statistical significance was determined by using the nonparametric combination test (Fig 2, *A* and *D*) or nonparametric 1-way ANOVA with the Dunn posttest (Fig 2, *B*, *C*, and *E*). * $P < .05$, ** $P < .01$, and *** $P < .001$. All data depicted are means \pm 6 SDs.

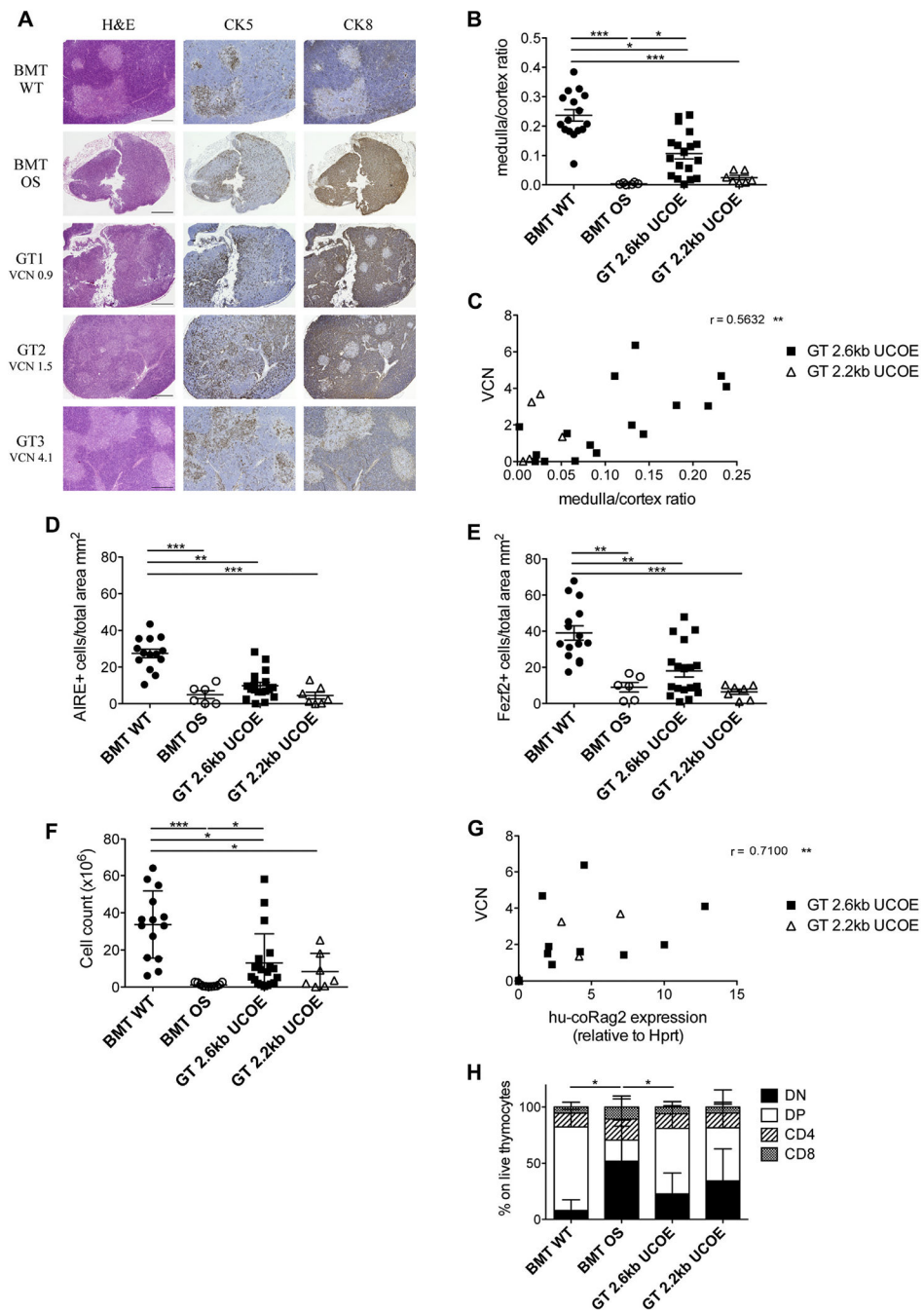


FIG 3. Thymic characterization. **A**, Histologic analysis of thymic sections stained with hematoxylin and eosin (*H&E*), cytokeratin (*CK*) 5, and cytokeratin 8 of representative BMT WT, BMT OS, and GT 2.6kbUCOE mice. VCN in the thymus is indicated for GT mice. *Scale bar* = 500 μ m. **B**, Ratio between the thymic medullary and cortical areas. **C**, Correlation between the medulla/cortex ratio and VCN of GT 2.6kbUCOE (*squares*) and GT 2.2kbUCOE (*triangles*) mice. The Spearman *r* value is indicated. **D**, Counts of AIRE⁺ cells in analyzed thymic sections (in square millimeters). **E**, Counts of Fexf2⁺ cells in analyzed thymic

sections (in square millimeters). **F**, Thymic cellularity (cell counts). **G**, Correlation between VCN and vector-induced human codon-optimized Rag2 (*hu-coRag2*) expression in thymocytes of GT 2.6kbUCOE (*squares*) and GT 2.2kbUCOE (*triangles*). Spearman *r* values and statistical significance are indicated. **H**, Distribution of double-negative (*DN*), double-positive (*DP*), and single-positive CD4 and CD8 cells in thymi (means \pm SDs). BMT WT mice, n = 16; BMT OS mice, n 5 10; GT 2.6kbUCOE mice, n = 20; GT 2.2kbUCOE mice, n = 6. Statistical significance was determined by using the nonparametric 1-way ANOVA with the Dunn posttest (Fig 3, *B* and *D-F*) by using Spearman correlation (Fig 3, *C* and *G*) or the nonparametric combination test (Fig 3, *H*). *P < .05, **P < .01, and ***P < .001. Error bars represent SDs.

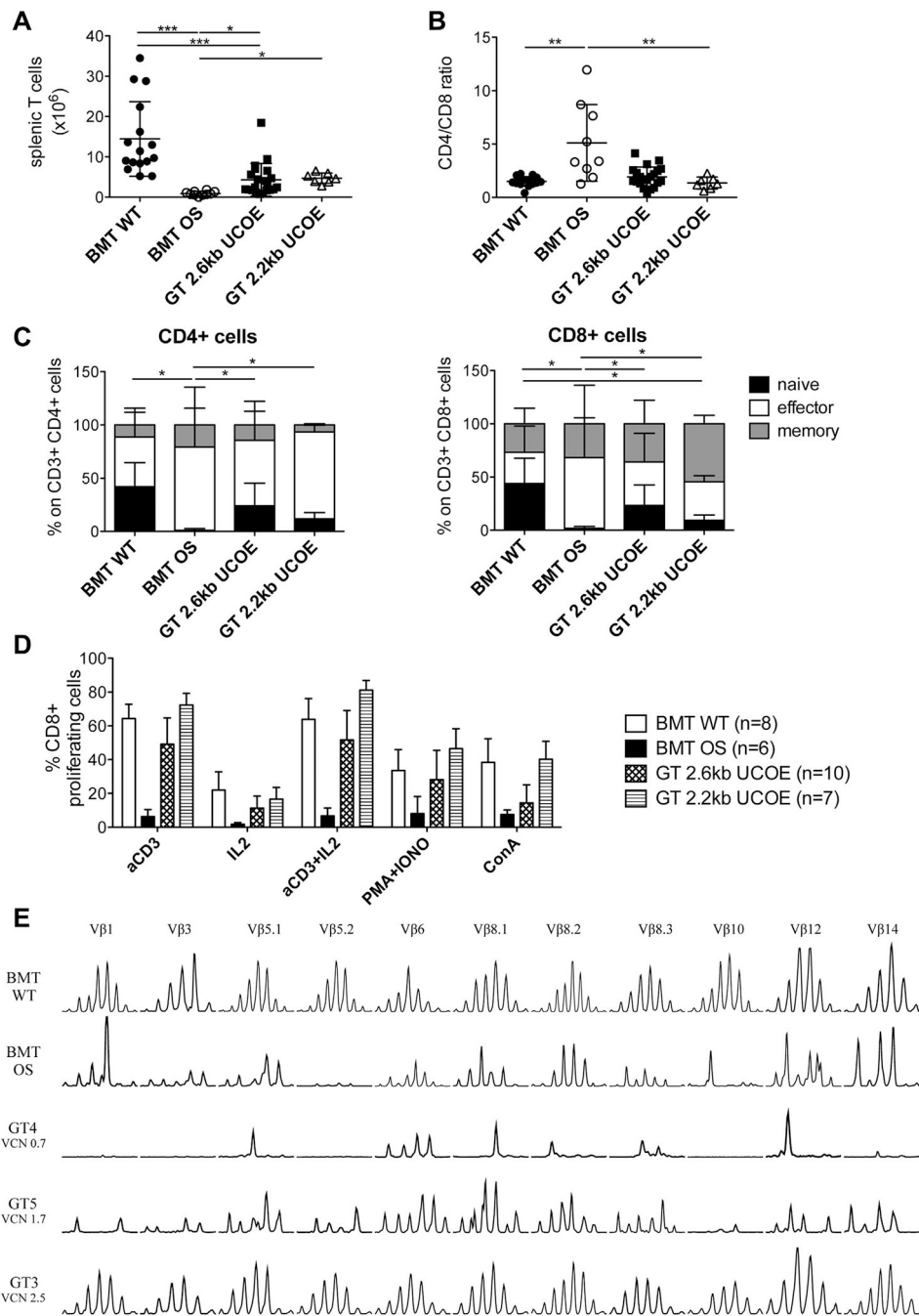


FIG 4. T-cell development and functionality. **A**, Absolute counts of T cells. **B**, Ratio between CD4⁺ and CD8⁺ T cells. **C**, Distribution of naive, effector, and memory subpopulations in CD4⁺ (left) and CD8⁺ (right) T cells. BMT WT mice, n = 16; BMT OS mice, n = 9; GT 2.6kbUCOE mice, n = 21; GT 2.2kbUCOE mice, n = 7. **D**, Percentage of CD8⁺ T cells that proliferate in response to the indicated stimuli. **E**, TCR repertoire analysis in spleen cells. Eleven Vβ families of representative BMT WT, BMT OS, and GT 2.6kbUCOE mice (with low, medium, and high VCN) are shown. Statistical significance was determined by using

nonparametric 1-way ANOVA with the Dunn posttest (Fig 4, *A* and *B*) or the nonparametric combination test (Fig 4, *C*). * $P < .05$, ** $P < .01$, and *** $P < .001$. All data show means \pm SDs.

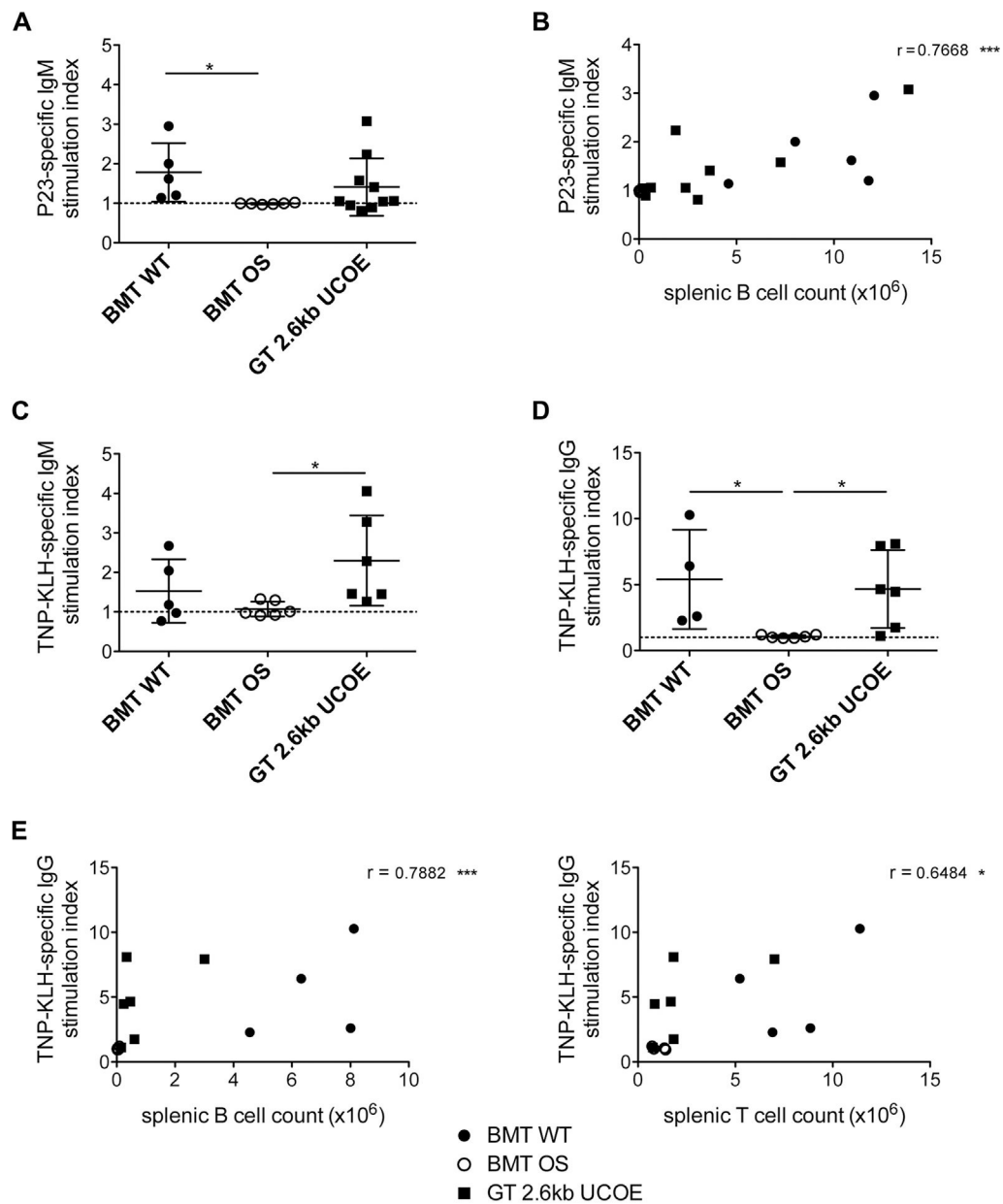


FIG 5. *In vivo* challenges. **A**, Stimulation index of Pneumovax-specific IgM calculated as the ratio of IgM produced at day 21 after vaccination and before immunization. **B**, Correlation between stimulation index of Pneumovax-specific IgM and absolute count of splenic B cells in BMT WT (*solid circles*), BMT OS (*open circles*), and GT 2.6kbUCOE (*squares*) mice. The Spearman r value is indicated. **C**, Stimulation index of TNP-KLH-specific IgM calculated as the ratio of IgM produced 21 days after immunization and before immunization. **D**, Stimulation index of TNP-KLH-specific IgG calculated as the ratio of specific IgG produced at day 28 and before the boosting dose. **E**, Correlation between the stimulation index of TNP-KLH-specific IgG and absolute count of splenic B (*left*) or T (*right*) cells. The Spearman r value is indicated for each graph. Statistical significance was

determined by using nonparametric 1-way ANOVA with the Dunn posttest (Fig 5, *A*, *C*, and *D*) or by using Spearman correlation (Fig 5, *B* and *E*). * $P < .05$ and *** $P < .001$. All data show means \pm 6 SDs.

Author Manuscript

Author Manuscript

Author Manuscript

Author Manuscript

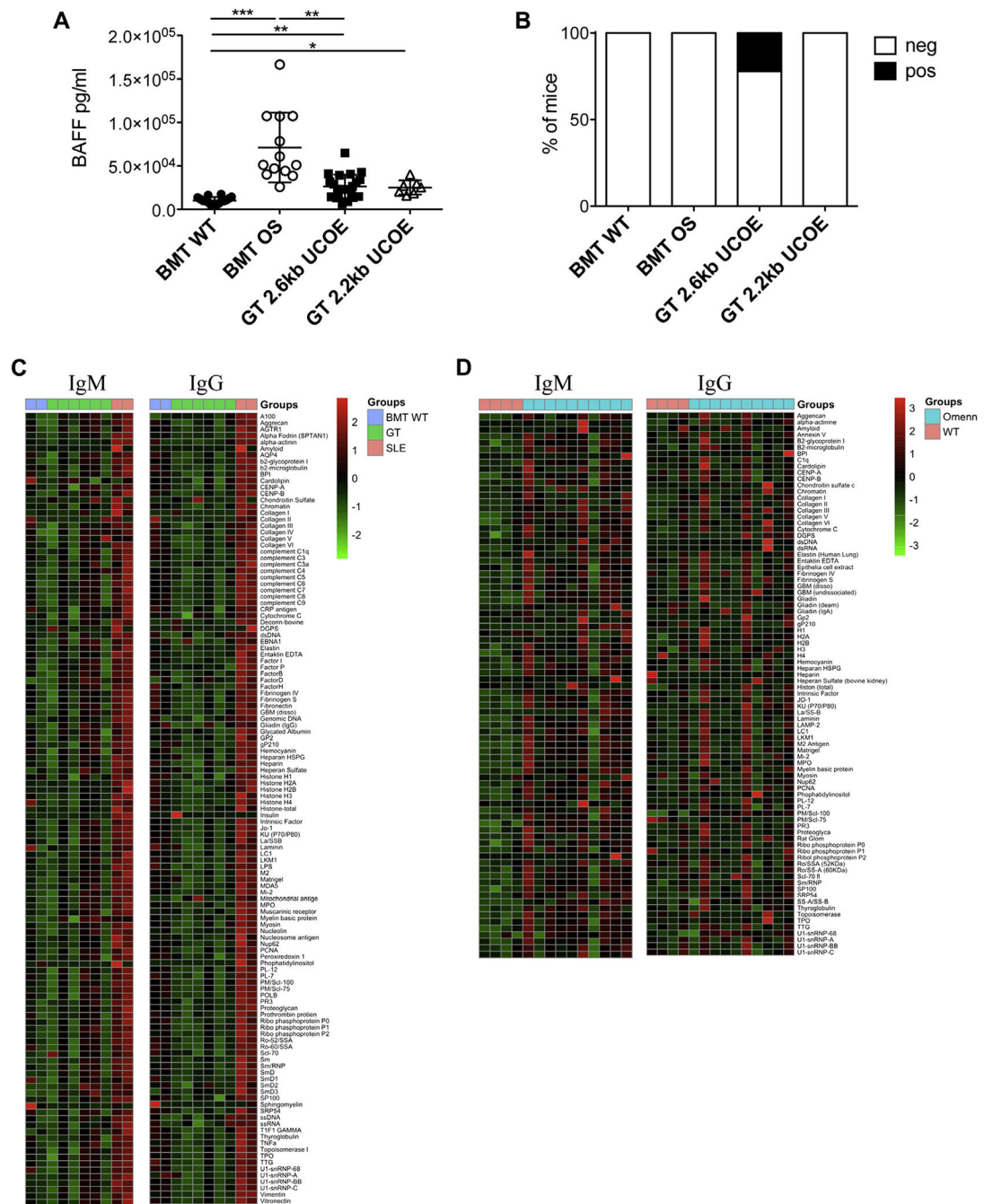


FIG 6. Autoimmune manifestations. **A**, BAFF levels in sera at the time of 28 weeks. Statistical significance was determined by using nonparametric 1-way ANOVA with the Dunn posttest. * $P < .05$, ** $P < .01$, and *** $P < .001$. **B**, Frequency of mice with the presence (white) or absence (black) of anti-double-stranded DNA autoantibodies in sera (BMT WT mice, $n = 14$; BMT OS mice, $n = 10$; GT 2.6kbUCOE mice, $n = 18$; GT 2.2kbUCOE mice, $n = 5$). **C**, Heat map representation of relative autoantibody IgM and IgG reactivity against 123 antigens tested in BMT WT, GT, and systemic lupus erythematosus (SLE) mice. Colors

correspond to normalized (z-score) expression levels. **D**, Heat map representation of relative autoantibody IgM and IgG reactivity against 86 antigens tested in untreated WT and OS mice. Colors correspond to normalized (z-score) expression levels.

Author Manuscript

Author Manuscript

Author Manuscript

Author Manuscript

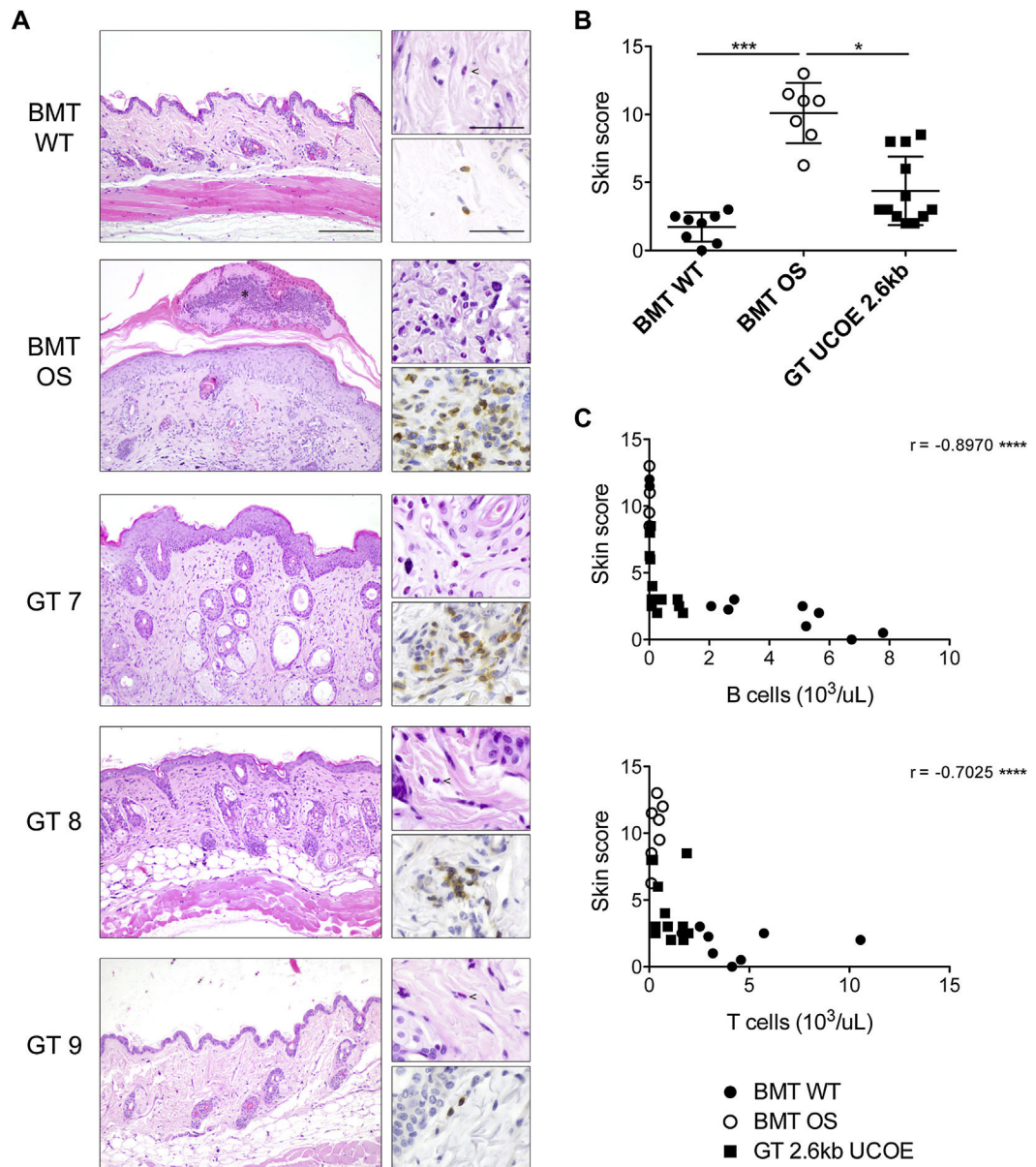


FIG 7. Skin infiltration. **A**, Histologic analysis of skin sections stained with hematoxylin and eosin (*left*) of representative BMT WT, BMT OS, and GT 2.6kbUCOE mice. *Upper right*, Eosinophils are visible at higher magnification; *lower right*, T-cell infiltration is shown in CD3-stained sections. *Scale bars* = 200 μ m (*left*) and 50 μ m (*right*). **B**, Arbitrary score of skin manifestations calculated as described in the Methods section. **C**, Correlation between skin infiltration score and absolute count of B (top) and T (bottom) cells in the peripheral blood of BMT WT (*solid circles*), BMT OS (*empty circles*), and GT 2.6kbUCOE (*squares*) mice. The Spearman *r* value is indicated for each graph. Statistical significance was determined by using nonpara-metric 1-way ANOVA with the Dunn posttest (Fig 7, **B**) or by using Spearman correlation (Fig 7, **C**). **P* < .05, ***P* < .01, ****P* < .001, and *****P* < .0001.

TABLE I.

Main outcomes of OS GT

Outcomes	Untreated OS mice	OS mice after GT
B-cell counts	Absent or very low	Improved but lower than BMT WT mice
B-cell phenotype	Blocked at early stage of differentiation	Normal maturation
T-cell counts	Strongly reduced	Improved but lower than BMT WT mice
T-cell phenotype	Highly activated and exhausted with oligoclonal skewed repertoire	Presence of naive cells, able to respond to stimuli and with skewed to polyclonal phenotype
IgM and IgG levels	Very low	Normal
IgE levels	Normal to high	Normal
Thymus	Absence of medulla; very low thymocyte counts	Low to normal medullary area, in correlation with VCN; improved thymocyte counts
Vaccination response	Unable to respond to vaccination	Able to mount proper antigen response
Autoantibodies	Low to high	Low or absent
Skin infiltration	Moderate to severe	Absent to moderate

Author Manuscript

Author Manuscript

Author Manuscript

Author Manuscript